2D Modelling of Carbon Steel Microstructure Including Hardening Elements.

ADEMOLA O. ISRAEL[1], OLULEKE O. OLUWOLE[2], ADELUSI I. S[3], O. O. AJIDE[4]
[1, 2, 3, 4] *University of Ibadan*

Abstract- The microstructure of the low carbon steel has been researched most time without considering its trace elements how it contributes to its mechanical properties. This research was able to consider the mechanical properties of the trace elements in the pearlite face (as a composite) to give a proper stress-strain values which is used to validate the young modulus of low carbon steel in literature. The microstructure used was a 2D & 3D Voronoi tessellation model from MATLAB where the surface plot was done and then exported to ANSYS for proper stress analysis. Comparing the FEA results and low carbon steel young's modulus of literature, maximum value of 192.22GPa was recorded in sample. It then gives a better prediction of the stress-strain values by embedding the property of the trace elements in the base property of the 0.25 wt.% low carbon steel. However, the analysis shown that the trace elements contribute to the stress-strain values of the model which is close to that of low carbon steel with about just 4% deviations. This therefore affirms the significance of the hardening (trace) elements contributing to the behavior of Carbon in the microstructure

I. INTRODUCTION

Micro-defects (voids, cracks etc.) resulting from manufacturing and operational processes have existed in engineering structures since the dawn of time. As a result of combined loading and environmental circumstances, this flaw might spread throughout the material, resulting in catastrophic failure. Meanwhile, understanding microstructural phenomena as well as structural components, is essential to materials selection, design, and durability. Metals and alloys exhibit complex mechanical behavior at high temperatures due to the combination of time and temperature dependent processes. (Aghogho et al., 2020) [1] said in order to determine the mechanical behavior of low carbon steel material and to acquire the stress value for different low carbon steel samples when exposed to tensile test, a tensile testing equipment known as universal testing machine can be used. Low carbon steels consist primarily of ferrite, which is a solid solution phase of carbon dissolved in alpha-iron, a body centered cubic crystal (BCC). Low-carbon steels contain up to 0.30% carbon. A majority of this class of steel is flat-rolled products like sheet or strip; usually they are in a cold-rolled and annealed condition.

Using a 2D microstructure implies that it is modelled as a plate. This study will aid in a better understanding of the behavior of low carbon steel to strain taking into consideration the trace elements. This understanding will aid in the design and development of high-performance materials by allowing for careful control of the steel's microstructure. (Oluwole et al., 2017) [2] discovered that previous Voronoi models using line plots could not be exported from MATLAB to ANSYS workspace because the formats were incompatible. As a result, the model was remodeled using surface plots and divided into two aspects: ferrite and pearlite. (Ankamma, 2014) [3] attempted to correlate the Effect of trace elements (B and Pb) on the tensile strength, hardness, and microstructure of gray cast iron. These elements have a large impact on the properties and microstructure of gray cast iron. (Kumar et al., 2022) [4] used Stir-casting to make Al-5.6Zn-2.2Mg-1.3Cu composites with particle sizes ranging from 30 to 90 m and weight fractions ranging from 5 to 15 SiC articles. The material's mechanical and wear properties have been evaluated. (Ali et al., 2021) [5] investigated the effect of boron and boron with niobium additions on the phase transformation behavior, microstructures, and mechanical properties of thermos-mechanically controlled hot-rolled and direct-quenched low-carbon bainitic steel plates. The investigation of low-carbon bainitic steel plates. (Liu et al., 2023) [6] studied the influence of Sn on the microstructure of the Fe-0.05wt%, C-0.03wt%, Si-

1.28wt%, Mn-0.36wt%, S-0.05wt%, P base composition containing 0.0002 (without addition), 0.062, 0.12, and 0.18 Sn (wt.%) low-carbon free-machining steels using thermodynamic calculations, optical microscopy, scanning electron microscopy, transmission electron microscopy, electron probe microanalysis, and high-temperature laser scanning confocal microscopy. (Yu, 2017) [7] investigated that Boron addition had an effect on the microstructure and mechanical properties of a low-carbon cold rolled enamel steel. Boron addition had an effect on the microstructure and mechanical properties of a low-carbon cold rolled enamel steel. (Srivastava & Verma, 2016) [8] investigated the effect of particles on the mechanical properties of epoxy resin, copper and aluminum particles reinforced epoxy resin was created in this study (PL-411). Copper (Cu) and aluminum (Al) particles were added as fillers to epoxy resin in varying weight percentages (1%, 5%, 8%, and 10%).

Different methods, including experiments and simulation calculation, have been used to study the constituent trace element mechanical behavior/properties. (Onurisi & Oluwole, 2011) [9] investigated the experimental and simulation study of the effects of stress on microstructure and failure morphology of low carbon steel under plane stress conditions. The research discovered significant grain extension at the point of fracture, as well as stress and strain looping around the pearlitic faces of the microstructure matrix. (Joseph & Alo, 2014) [10] investigated the effect of heat treatment on the microstructure and mechanical properties of 0.26% low carbon steel at 850^{0}C using various cooling media. Heat treatments such as annealing, normalizing, and age-hardening were used in the experiment. (Oluwole et al., 2017) [2] modeled microstructures were subjected to a line load on one of their edges while the opposite edge was fixed. This resulted in a displacement of the geometry from its original position. Stress and strain results were also observed. (Kantor et al., 2020) [12] used multiple impact toughness tests and electron backscatter diffraction microstructure measurements were used to establish a link between the occurrence of remarkable impact toughness scattering in the ductile-to-brittle transition region and microstructure features of low carbon micro-alloyed steel. (Boumerzoug, 2017) [13] uses the following techniques to achieve the goal: optical microscopy, EBSD, X-ray diffraction, and hardness tests. Several zones and phases have been identified. The EBSD technique is used to observe new microstructural phenomena. (Ron et al., 2019) [14] uses Tension testing and hardness measurements were used to assess mechanical properties, while scanning electron microscopy and X-ray diffraction analysis to assess microstructure. Salt spray testing, immersion testing, potentiodynamic polarization analysis, and electrochemical impedance spectroscopy were used to assess general corrosion performance. Slow strain rate testing was used to characterize stress corrosion performance (SSRT).

II. PREPARATION OF THE LOW CARBON STEEL

The low carbon steel material geometry is a cylindrical rod, having a diameter of 12mm and 450mm long. steel material to tension in the Universal Testing Machine (UTM). Its maximum tensile stress is 275.82MPa, its load at maximum tensile force is 48.74kN, tensile strain at maximum tensile strain is 0.0011256.

The low carbon steel material composition used is shown below:

Table 1: composition of low carbon steel material.

Elements	Wt. %
Titanium (Ti)	0.0006
Copper (Cu)	0.0147
Molybdenum (Mo)	0.0054
Vanadium (V)	0.0007
Cobalt (Co)	0.0042
Aluminum (Al)	0.0440
Antimony (Sb)	0.0008
Nickel (Ni)	0.0460
Carbon (C)	0.2490
Manganese (Mn)	0.2110
Chromium (Cr)	0.0820
Silicon (Si)	0.0050
Iron (Fe)	99.3537

2.1 Strain Rate

Strain rate is the measures rate of deformation, its precise definition depends on how strain is measured.

$$\epsilon(t) = \frac{L(t) - L_0}{L_0} \quad (1)$$

Where Lo is the original length and L(t) is length at each time t. Then the strain rate will be

$$\dot{\epsilon}(t) = \frac{d\epsilon}{dt} = \frac{d}{dt}\left(\frac{L(t) - L_0}{L_0}\right) = \frac{1}{L_0}\frac{dL(t)}{dt} = \frac{v(t)}{L_0} \quad (2)$$

where v(t) is the speed at which the ends are moving away from each other. When the material is subjected to parallel shear without volume change, the strain rate can also be expressed as a single number; that is, when the deformation can be described as a set of infinitesimally thin parallel layers sliding against each other in the same direction as if they were rigid sheets, without changing their spacing. Then the strain in each layer can be expressed as the limit of the ratio between the current relative displacement of a nearby layer, divided by the spacing between the layers:

$$\epsilon(y,t) = \lim_{d\to 0}\frac{X(y+d,t) - X(y,t)}{d} = \frac{\partial X}{\partial y}(y,t) \quad (3)$$

the strain rate is

$$\dot{\epsilon}(y,t) = \left(\frac{\partial}{\partial t}\frac{\partial X}{\partial y}\right)(y,t) = \left(\frac{\partial}{\partial y}\frac{\partial X}{\partial t}\right)(y,t) = \frac{\partial V}{\partial y}(y,t) \quad (4)$$

where V(y,t) is the current linear speed of the material at distance y from the wall.

2.2 Average Equation of Composite

The composite microstructure will have an averaging composite equation for the pearlite phase of the microstructure as shown below:

Weight = mass × gravity (5)

$$\text{Volume} = \frac{\text{weight}}{\text{gravity} \times \text{density}} \quad (6)$$

Where g = 9,8m/sec squared. Acceleration due to gravity

$$\text{Volume Fraction} = \frac{\text{weight fraction}}{\text{gravity} \times \text{density}} \quad (7)$$

The volume, which takes 100 grams of composite material (we assume the material is non-porous). Meanwhile we will be using specific gravity to do away with gravity in our calculations.

$$\text{Total volume} = \frac{wt.\%\ of\ element\ a}{specific\ gravity\ of\ element\ a} + \frac{wt.\%\ of\ element\ b}{specific\ gravity\ of\ element\ b} + \cdots \quad (8)$$

Generally,

$$Volume\ Fraction\ of\ each\ elements = \frac{wt.\%\ of\ each\ elements}{specific\ gravity}\ x\ \frac{1}{\text{Total volume}}$$

(9)

Therefore:

$$\text{Average Equation of composite} = \frac{fraction\ vol.a*p + fraction\ vol.b*p + ...fraction\ vol.z*p}{Total\ Volume}$$

(10)

Where

- p are the mechanical properties i.e., yield strength, ultimate tensile strength and young modulus.
- a, b, c…, z are the trace elements.

III. MODEL AND SIMULATION

3.1 Generation of Microstructure Model Using Voronoi Tessellation

The mass fractions of proeutectoid ferrite and pearlite that form in a 0.25 wt. % C iron-carbon alloy is considered below using lever rule:

$$W_p = \frac{C_0' - 0.022}{0.74} = \frac{0.25 - 0.022}{0.74} = 0.31$$

for proeutectoid ferrite:

$$W_{\alpha'} = \frac{0.76 - C_0'}{0.74} = \frac{0.76 - 0.25}{0.74} = 0.69$$

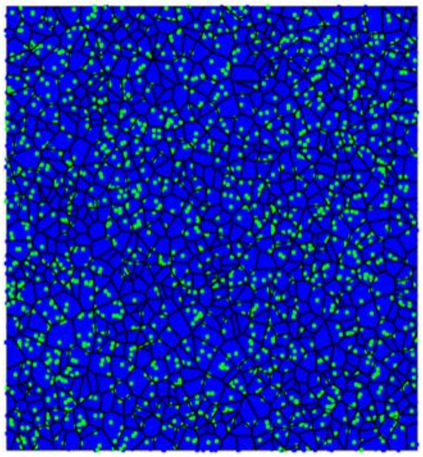

Figure 1: Both Ferrite and Pearlite Voronoi model microstructure (SVG).

3.2 Export Models to Space-claim to Edit Geometry and Conversion to Parasolid.

The model was exported to Space-claim and consequently to ANSYS Spaceclaim for Parasolid as shown below: For it to be Parasolid, it was extruded to about 10mm wide. The figure below shows the microstructure exported into ANSYS Space claim

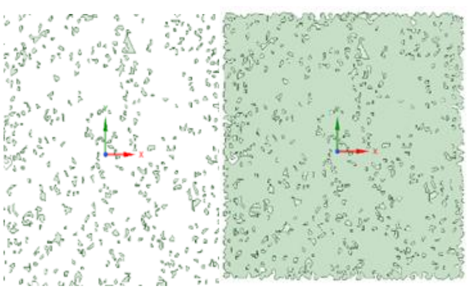

Figure 2: (a) 2D model of both Pearlite and Ferrite (b) Pearlite in Space-claim

3.3 Export to ANSYS for Stress Analysis

Static Structural was selected because the object under study needed to be of short time effect on the microstructure which is nonlinear to give a more precise strain hardening analysis. The model was embedded with pure trace elements (Silicon, Sulphur, Molybdenum, Manganese and so on) each in different occasions of the analysis in the ANSYS workbench/mechanical. The constituent elements mechanical properties are shown in the (Table 2), (Figure 2). The engineering property used for the microstructure is shown in (Table 3) (Figure 3)

Table 2: Material Properties for the Low Carbon Steel Model

Property	Yield Strength (MPa)	Tensile Strength (MPa)	Modulus (GPa)
Titanium (Ti)	450	520	120
Copper (Cu)	69	200	130
Molybdenum (Mo)	565	655	330
Vanadium (V)	454	536	125.5
Cobalt (Co)	225	800	207
Aluminum (Al)	35	90	70.5
Antimony (Sb)		11.4	77.75
Nickel (Ni)	138	480	190
Carbon (C)	415	620	24.5
Manganese (Mn)	241	496	159
Chromium (Cr)	131	550	279
Silicon (Si)	165	170	150
Iron (Fe)	50	540	200

Voronoi model is meshed by first converting the microstructure to solid state in Space-claim instead of faces as it is imported from MATLAB.

Table 3: Material Properties for the microstructure (LCS)

Property	Ferrite	Pearlite
Young's Modulus	200GPa	1.911GPa
Poisson's Ratio	0.3	0.3
Mass Density	7.85E +03kg/m	5.428E +01kg/m
Bulk Modulus	1.667E +11Pa	1.593E+09 Pa
Shear Modulus	7.692E +10Pa	7.350E+08 Pa
Tensile Strength	2.50E+08Pa	8.011E+6Pa
Ultimate Tensile Strength	4.6 E+08Pa	10.259E+6Pa

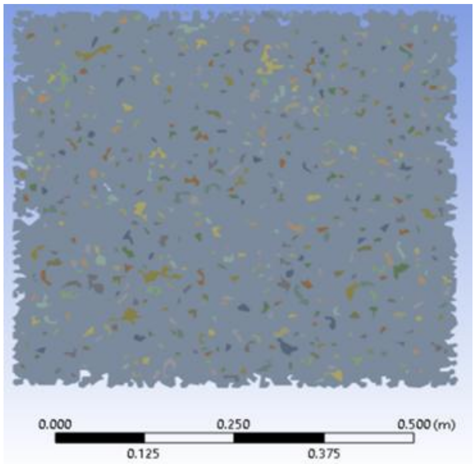

Figure 3: Ferrite and Pearlite Model Loaded into ANSYS (0.261%C).

The microstructure model is first constrained at one end and then both ends are subjected to displacement. The microstructure however was subjected to uniaxial loading. The following assumptions are also applied:

- The body force is negligible; hence it is neglected.
- Gravitational force is also negligible; it is neglected.
- The microstructure also is subjected to a pane strain condition.

IV. NUMERICAL RESULTS

The values show the strain impact with time when subjected to loading. It shows the greatest impact is experienced close to the force that subject the microstructure to tension. The time of simulations is six seconds. The maximum strain is 0.000645 (Figure 6). The results below show the stress-time of the simulation during the analysis. This shows that the stress increases with time and it doesn't exceed the yield stress. The maximum stress in elastic is 124 MPa (Figure 7).

The stress-strain graph is used to evaluate the tension test experimentation and anticipate the mechanical behavior under elastic straining for low carbon steel materials. The stress-strain is produced and the young modulus is investigated to be compared with literature (Figure 8) (Table 4).

V. DISCUSSIONS

From literature, the young modulus of a low carbon steel is 200GPa. This research takes into consideration the effect of the trace elements of the low carbon steel composition to get a better mechanical property for proper choice of material for different purposes.

This research compared with (Oluwole et al., 2017) [6] shows the trace elements considered will contribute to the perfect strain response when subjected to stress.

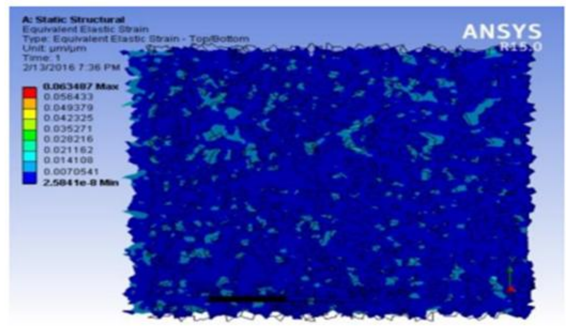

Figure 4: model without the trace elements considered

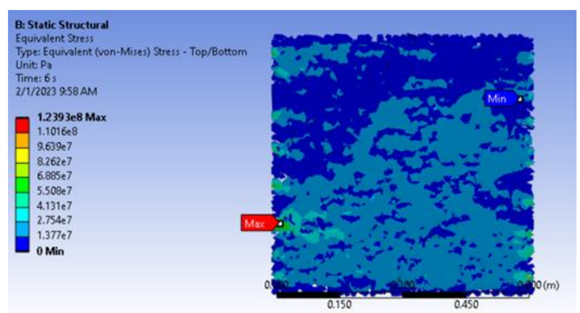

Figure 5: Model with trace element considered

Average of all the trace elements property was inputted into the 31% pearlite phase of the microstructure model. This then give us a modulus of 192.2558GPa which compared to (Oluwole et al., 2017) is close to the 200 GPa in literature with just about 3.87% deviation.

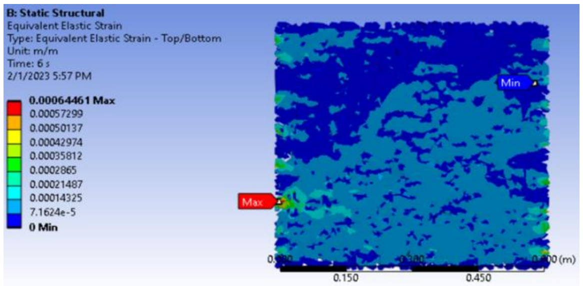

Figure 6: Strain values Results showing the maximum and minimum Strain

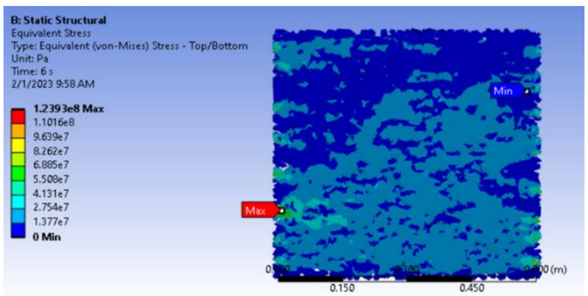

Figure 7: Equivalent Stress values Results showing the maximum and minimum Stress

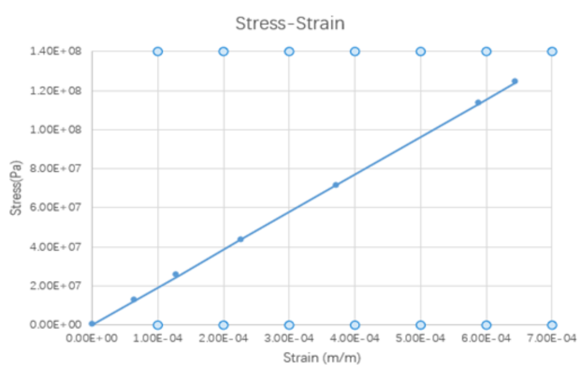

Figure 8: Stress-Strain plot from simulation.

Table 4: Stress- Strain values from Simulations

Stress [Pa]	Total Strain [m/m]
0.00E+00	0.00E+00
1.24E+07	6.45E-05
2.48E+07	1.29E-04
4.34E+07	2.26E-04
7.13E+07	3.71E-04
1.13E+08	5.88E-04
1.24E+08	6.45E-04

VI. DISCUSSIONS

The young modulus from the stress-strain values from analysis validates that

1. the 2D Voronoi model of the ferrite pearlite taking into consideration the trace element contributes to give the microstructure a better mechanical property.
2. This gives us a better prediction during the elastic straining of the low carbon steel.
3. The low carbon steel straining can then give a better stress-strain response and a desired material without changing the configuration or permanent deformation during strain variation.

REFERENCES

[1] Aghogho, O. T., Akanni, A. A., Olayiwola, A. J., Ikubanni, P. P., & Odusote, J. K. (2020). Microstructural image analyses of mild carbon steel subjected to a rapid cyclic heat treatment. Journal of Chemical Technology and Metallurgy, 55(1), 198–209.

[2] Oluwole, O. O., Oguntokun, O. A., Obi, H. N. O. C., & Fajobi, M. (2017). Stress Analysis of MATLAB Developed Voronoi Microstructure Models using ANSYS Stress Analysis of MATLAB Developed Voronoi Microstructure Models using ANSYS . July, 1–5.

[3] Ankamma, K. (2014). Effect of Trace Elements (Boron and Lead) on the Properties of Gray Cast Iron. 95(June), 19–26. https://doi.org/10.1007/s40033-013-0031-3

[4] Kumar, R., Jha, K., Sharma, S., Kumar, V., & Li, C. (2022). Heliyon Effect of particle size and weight fraction of SiC on the mechanical , tribological , morphological , and structural properties of. 8(September). https://doi.org/10.1016/j.heliyon.2022.e10602

[5] Ali, M., Nyo, T., Kaijalainen, A., Javaheri, V., Tervo, H., Hannula, J., Somani, M., & Kömi, J. (2021). Incompatible effects of B and B + Nb additions and inclusions' characteristics on the microstructures and mechanical properties of low-carbon steels. Materials Science and Engineering A, 819(March). https://doi.org/10.1016/j.msea.2021.141453

[6] Liu, X., Han, Y., Wei, J., Zu, G., Zhao, Y., Zhu, W., & Ran, X. (2023). Jo ur n re. Journal of

Materials Research and Technology. https://doi.org/10.1016/j.jmrt.2023.01.061
[7] Yu, B. (2017). ScienceDirect ScienceDirect Influence of boron addition on microstructure and properties of a low-carbon cold rolled enamel steel. https://doi.org/10.1016/j.proeng.2017.10.947
[8] Srivastava, V. K., & Verma, A. (2016). Mechanical Behaviour of Copper and Aluminium Particles Reinforced Epoxy Resin Composites. April. https://doi.org/10.5923/j.materials.20150504.02
[9] Onurisi, N. O., & Oluwole, O. (2011). Stress effects on microstructure and failure morphology of low carbon steel sheet. Leonardo Electronic Journal of Practices and Technologies, 10(19), 118–132.
[10] Joseph, O. O., & Alo, F. I. (2014). An Assessment of the Microstructure and Mechanical Properties of 0 . 26 % Low Carbon Steel under Different Cooling Media : Analysis by one-way ANOVA. 4(7), 39–46.
[11] Joseph, O. O., & Alo, F. I. (2014). An Assessment of the Microstructure and Mechanical Properties of 0 . 26 % Low Carbon Steel under Different Cooling Media : Analysis by one-way ANOVA. 4(7), 39–46.
[12] Kantor, M. M., Vorkachev, K. G., Bozhenov, V. A., & Solntsev, K. A. (2020). The microstructure of low carbon microalloyed steel and impact toughness scattering during fracture in ductile-to-brittle transition region. Procedia Structural Integrity, 30, 45–52. https://doi.org/10.1016/j.prostr.2020.12.009
[13] Boumerzoug, Z. (2017). Effect of Welding on Microstructure and Mechanical Properties of an Industrial Low Carbon Steel. January 2010. https://doi.org/10.4236/eng.2010.27066
[14] Ron, T., Levy, G. K., Dolev, O., Leon, A., Shirizly, A., & Aghion, E. (2019). Environmental behavior of low carbon steel produced by a wire arc additive manufacturing process. Metals, 9(8). https://doi.org/10.3390/met9080888